Freeze-thaw durability of conventional and a novel permeable pavement replacement

Alalea Kia*, Ph.D.; Hong S. Wong, Ph.D.; Christopher R. Cheeseman, Ph.D.

Department of Civil and Environmental Engineering, Imperial College London, SW7 2AZ, UK

*Corresponding author: alalea.kia@imperial.ac.uk

Abstract

Permeable concrete pavements are becoming more common as a stormwater management system to mitigate urban flooding. However, they have a number of well-defined drawbacks including low permeability, high clogging potential, and low strength and durability, notably in cold climates exposed to freezing and thawing. A new generation of high-strength clogging resistant permeable pavement replacement (CRP) has been developed, through extensive laboratory work, to address these shortcomings and advance the field of permeable pavements. This paper reports on new advances in permeable pavement systems and the performance of a range of conventional permeable concrete and the developed novel CRP of varying porosity exposed to freeze-thaw cycles. This will allow performance evaluations of both systems in a cold climate. The tests involved exposing samples to temperature varying from -20^{o}C to +20^{o}C and measuring changes in mass, area, compressive strength and ultrasonic pulse velocity after each cycle. These new results show that CRP is highly resistant to degradation caused by freeze-thaw cycles compared to conventional permeable concrete, reducing maintenance requirements and improving service-life. This study presents the first high strength clogging resistant permeable pavement replacement that is durable under frost action, these findings will support and enable wider use of permeable pavements in cold regions.

Keywords: Permeable concrete; frost; durability; flooding; clogging resistant; high strength

Introduction

In recent years, permeable pavements are extensively promoted as a mitigation strategy for urban flooding. These highly porous materials rapidly drain surface water, enabling storm water to pass through dense infrastructure. However, conventional permeable pavements are inevitably prone to clogging, due to their indirect pore channels that are highly tortuous and heterogenous, degrading their performance and service life (Chopra *et al.*, 2007; Deo *et al.*, 2010; Schaefer & Kevern, 2011; Coughlin *et al.*, 2012; Kayhanian *et al.*, 2012; Mata & Leming, 2012; Yong *et al.*, 2013; Kia *et al.*, 2017; Kia *et al.*, 2018; Kia *et al.*, 2019). Clogging is caused by build-up of debris trapped within the pore network, blocking the pavement and reducing its drainage capacity. Further details are presented in Kia *et al.* (2018) and Kia *et al.* (2017). Conventional permeable pavements also have low strength (<30 MPa), owing to their high porosity (15%-35%), and are limited to light applications (Kim & Obla, 2009; Kevern *et al.*, 2010; Lian & Zhuge, 2010; Sumanasooriya & Neithalath, 2011; Sumanasooriya *et al.*, 2012; Sonebi & Bassuoni, 2013). Although the use of permeable concrete pavements is expanding, their application in cold regions has been limited due to concerns of deterioration under frost action (Schaefer *et al.*, 2006).

A number of studies have found that addition of fine aggregates and polypropylene fibres improves strength and enhances resistance to freeze-thaw (F-T) degradation but it reduces porosity and permeability which are the main contributors to the pavement's overall drainage performance (Yang & Jiang, 2003; Schaefer *et al.*, 2006; Kevern, 2008; Kevern *et al.*, 2008a; Kevern *et al.*, 2008b; Kevern *et al.*, 2010; Yang, 2011; Huang *et al.*, 2012; Amde & Rogge, 2013; Bonicelli *et al.*, 2015; Bilal *et al.*, 2021). Addition of rubber to pervious concrete mixes has been shown to decrease porosity and permeability, but to improve freeze-thaw resistance (Gesoğlu *et al.*, 2014; Mondal & Biligiri, 2018; Liu *et al.*, 2018a). Adding silica fume (up to 5% wt. cement paste) improves workability and enhances F-T resistance but it reduces porosity (Kevern *et al.*, 2008b; Yang, 2011). However, increasing the replacement rate (>5% wt. cement paste) will lead to a dry mixture that is difficult to

compact, resulting in increased porosity and reduced F-T durability (Kevern *et al.*, 2008b). The aggregate type used in permeable concrete was also found to influence F-T deterioration, aggregates with specific gravity >2.5 and absorption <2.5% are more durable (Kevern *et al.*, 2008a; Kevern *et al.*, 2008b; Kevern *et al.*, 2010). Increasing compaction improves resistance to F-T degradation and surface ravelling, but this reduces porosity and drainage performance (Schaefer *et al.*, 2006; Kevern *et al.*, 2008a; Kevern *et al.*, 2008b; Henderson & Tighe, 2012; Bilal *et al.*, 2021). Permeable concretes with porosity <15% are durable, but those with porosity >30% exhibit poor F-T resistance (Kevern *et al.*, 2008a; Kevern *et al.*, 2008b; Liu *et al.*, 2018b). Air entrainment is also known to improve F-T resistance of permeable concrete pavements by decreasing the hydraulic pressure that develops during freezing of pore water (Schaefer *et al.*, 2006; Kevern *et al.*, 2008a; Kevern *et al.*, 2008b; Kevern *et al.*, 2010; Henderson & Tighe, 2012). However, the presence of entrained air voids can lead to further reductions in compressive strength.

Clogging accelerates F-T degradation of permeable concrete pavements because trapped water expands when it undergoes freezing (Tennis *et al.*, 2004; Yang *et al.*, 2006; Guthrie *et al.*, 2010; Izevbekhai & Akkari, 2011). This causes the thin layer of cement paste in conventional permeable concrete to crack and de-bond from the aggregate particles. Guthrie *et al.* (2010) evaluated the resistance of permeable concrete to F-T degradation at different levels of soil clogging and water saturation. Clogging was performed using poorly graded sand, with 11.7% by mass finer than 75 μm, collected from site to mimic field conditions and sieved to use the fraction <0.297 mm. It was found that specimens that were clogged and/or fully saturated deteriorated at a faster rate than those that remained unclogged and unsaturated. The average number of F-T cycles to failure was 93 for clogged specimens compared to 180 for unclogged specimens, and 80 for saturated specimens compared to 193 for unsaturated specimens. However, strength and stiffness measurements indicated no significant differences between the clogged and unclogged specimens. This was because only the

upper 25-50 mm of the 180 mm permeable concrete was filled with soil in clogged locations and the remaining depth was water free.

New types of permeable pavements have been developed to overcome the previously discussed limitations in conventional permeable pavements. Jones *et al.* (2010) developed concrete beams with drainage holes, 12.5 mm in diameter with 50 mm spacing and porosity of 3.1%. They compared the splitting tensile strength and modulus of rupture of these precast concrete beams, with equivalent beams without drainage holes. It was reported that the strength ratio between the beams with and without drainage holes was approximately 0.71. Jones *et al.* (2010), highlighted a number of issues in preparing these test specimens, including breakage of the vertical dowels.

A more recent development is high-strength clogging resistant permeable pavement (CRP), which improves upon the strength, drainage performance, and clogging resistance observed in conventional systems. This was achieved by engineering a uniform pore structure of low tortuosity (direct pore channels of 3 mm to 6 mm diameter) in self-compacting mortar. Rigorous lab testing supported by modelling confirmed its superior strength and drainage performance (Kia *et al.*, 2019). The new material has high strength (twice as strong as conventional pervious concrete pavements, >50 MPa) and high permeability (ten times more permeable than conventional pervious concrete pavements, >2 cm/s), yet does not clog despite extensive cyclic exposure to sand and clay. CRP is at least twice as strong and ten times more permeable than conventional permeable pavements of equal porosity, which completely clogged after just a few cycles of sediment exposure (Kia *et al.*, 2018; Kia *et al.*, 2019). The superior permeability and clogging resistance of CRP is due to the homogenous pore structure of constant cross-section and tortuosity of 1, allowing the water and sediments to flow through them without being trapped within the pore structure. The challenges of scaling up the innovation for flood prevention were addressed by developing a novel interlocking tile system (Kia *et al.*, 2020) which was recently deployed at scale as cast in-situ slab at the new White City Campus

of Imperial College London in United Kingdom (Fig. 1). This system was shown to be easier to construct at scale on site as unlike the conventional systems, it uses self-compacting cementitious material and does not require specialist contractors for placing it to avoid over-compaction or closing off of the surface pores (Kevern *et al.*, 2009; ACI., 2010; Kia *et al.*, 2017; Debnath & Sarkar, 2020). A structural and hydrological design methodology for this system has also been report in Kia *et al*. (2021).

The overall aim of this study is to: i) compare two different permeable pavement systems (conventional pervious concrete and CRP); ii) evaluate their strength and durability when exposed to cyclic freezing and thawing conditions; and iii) assess the benefits of the new permeable pavement replacement system and their widespread adoption. Experimental variables are aggregate particle size (1.25 mm to 14 mm), effective porosity (2% to 37%), pore diameter (3 mm to 6 mm) and the F-T degradation method used to simulate temperature and moisture gradients experienced in the field. The results are compared against conventional permeable concrete pavement subjected to the same F-T cycles. The data developed in this research will enhance our understanding of the performance of permeable pavements when exposed to cyclic freeze-thaw and enable practitioners to specify their wider use in cold climates.

Experimental program

Sample preparation

Two sample types were tested: a) conventional permeable concrete and b) high-strength clogging resistant permeable pavement. Seven conventional permeable concrete (PC) mixes were prepared using CEM I 52.5N Portland cement (100% cement with strength class of 52.5N) at water/cement (w/c) ratio of 0.35 and Thames Valley gravel. Thames Valley gravel consists of gravel and shingle with particle size ranging from 1.25 mm to 14 mm, a 24-h absorption of 1.76% and a specific gravity of 2.51. Mix proportions were based on the absolute volume method to achieve a target porosity of

16%-37%. In order to calculate the required paste volume, the target porosity was deducted from the packed aggregate void content and a 5% compaction index was added. The required cement and water contents were then calculated from the paste volume and w/c ratio. Finally, coarse aggregate content was calculated from the paste volume and target porosity. Trial mixing and testing found that this approach produced samples with measured void content close to the target porosity. Paste drain down was observed in two mixes and so a viscosity-modifying admixture (VMA) (MasterMatrix SDC) was added to these. In one case, VMA was added to achieve a higher porosity. Table 1 shows the PC mix proportions. Samples were cast in 100 mm cubic steel moulds and compacted in three equal layers for 25 sec each, using a vibrating table of adjustable intensity. This was determined from trials carried out to study the effect of compaction time on void content of packed Thames Valley gravel. In total, 42 PC samples were prepared.

Eight high-strength clogging resistant permeable pavement (CRP) with target porosity ranging from 2%-30% (Fig. 2) were prepared by introducing tubes of varying diameter (3 mm to 6 mm) and number into self-compacting mortar. Self-compacting mortar was prepared using CEM I 52.5N (711 kg/m^3) and fine-grained river sand (<2.5 mm, 1323 kg/m^3) at a w/c ratio of 0.40. The specific gravity of sand was 2.76 and 24-h absorption was 0.7%. A polycarboxylic-ether type superplasticiser (MasterGlenium 315C) was utilised at 0.25% wt. of cement to achieve the desired workability. Mix compositions of CRP are shown in Table 2. The number and size of the plastic tubes were varied in order to achieve different porosities. The CRP samples were cast in 100 mm cubic steel moulds, with the plastic tubes held in place using two steel meshes fixed at the top of the moulds. Overall, 48 CRP samples were prepared.

All control and F-T exposed CRP and PC samples were cast and cured in accordance with BS ISO 1920-3:2019 (British Standards Institution, 2019) covered with wet hessian and polyethylene sheet for the initial 24 hours. The F-T samples were de-moulded, weighed, wrapped in a plastic film (to

ensure that they are moisture-tight) and stored in a room at 20°C for 6 days. On the 7th day, the samples were removed from the plastic film, weighed and placed in a water bath (20°C) for 21 days. After 28 days (since casting), the specimens were removed from the water bath, surface dried with a towel and weighed. This value was used as the mass of the sample at cycle 0. The control samples were demoulded and placed in a fog room at 20°C, 95% ± 5% RH until they were tested for compressive strength. The excess protruding plastic tubes on the top surface of CRP samples were trimmed using a grinder in order to produce a flat surface for testing (Fig. 2).

Porosity

The porosity (ϕ) of conventional permeable concrete were determined from the mass of saturated-surface dry sample in air and in water as follows:

$$\phi = \left[1 - \frac{(W_3 - W_1)}{V \rho_w}\right] \times 100\% \quad (1)$$

where W_1 is the sample mass (kg) in water, W_3 is the saturated surface dry sample mass in air (kg), V is the sample volume (m^3) and ρ_w is the density of water (1000 kg/m^3). Before W_1 was measured, any trapped air was removed by keeping the sample submerged in water for a minimum of 30 minutes, inverting it and tapping it on a regular basis. Six replicate samples per mix were tested and the results averaged.

Porosity (ϕ) of CRP was calculated from the size and number of straight pores (plastic tubes) in the mix:

$$\phi = \left[\frac{V_p \times n}{V_c}\right] \times 100\% \quad (2)$$

where V_p is the volume of each pore, n is number of pores and V_c is the sample volume (m^3) (Kia *et al., 2019)*. Results were confirmed experimentally by filling the pores with water and dividing its volume by the volume of the sample. Porosity was recorded and averaged on 6 replicates per mix.

Cyclic freeze-thaw (F-T)

The F-T testing was conducted using the conventional testing method to enable comparison between the two permeable pavement systems (conventional permeable concrete and CRP). Samples were subjected to F-T testing in accordance with CEN/TR 15177:2006 (British Standards Institution, 2006) using three replicates per mix. Exposure was conducted under drained condition with one F-T cycle per day. This is considered less extreme compared to freezing under full saturation and more representative of the conditions encountered in the field for permeable concrete pavements (Attiogbe, 1996; NRMCA, 2004; Schaefer *et al.*, 2006; ACI., 2010). Each cycle consists of freezing at -20^{o}C for 8 hours followed by thawing in a water tank at +20^{o}C for 4 hours. The samples were manually moved between the freezer and the water tank due to the absence of an automated environmental chamber. After thawing, the saturated samples were surface dried with a towel, then weighed, scanned and tested for ultrasonic pulse velocity (UPV). The change in mass and UPV were measured to characterise deterioration rate under freezing and thawing cycles. All sides of the samples were imaged with a flatbed scanner (400 dpi) after every F-T cycle. Using digital image analysis, the scanned surfaces were analysed, using an image processing program (ImageJ), to determine the average area remaining (average taken from 4 sides of every sample, there were 3 replicates per mix) in each sample after each F-T cycle exposure. The area remaining was manually delineated for each cycle (approximately 500 × 500 pixels) and was calculated by dividing the area of the sample in each cycle by the original area determined in cycle 0 (prior to F-T exposure). The samples were exposed to a total of recommended 56 F-T cycles (British Standards Institution, 2006).

Ultrasonic pulse velocity

Ultrasonic pulse velocity was measured using Proceq Pundit (P-wave transducer, 54 kHz) in accordance with ASTM C597-16 (ASTM International, 2016) on three replicate samples per mix. Direct measurements were taken at five locations on each side of the cube excluding the top and bottom faces (i.e. 10 measurements per cube). Petroleum jelly was used as a coupling agent between the transducer and sample surface in order to achieve a stable UPV reading. Measurements were

carried out after every F-T cycle and the mean value was calculated to detect microstructural changes and potential degradation. Deterioration in the form of micro and macro cracking will increase the actual path length for the pulse to travel from transmitter to receiver compared to the assumed straight path. This increases the pulse propagation time, and therefore a causes reduction in the measured velocity.

Mass loss and durability factor

The percentage mass loss was calculated after every F-T cycle and this was used to determine the durability factor (DF) at mass loss of 2%, 3%, 4%, 5%, 6%, 8%, 10%, 12%, 15%, 18%, 20% and 25%. The DF is defined as (Wu *et al.*, 2016):

$$\mathrm{DF} = \frac{P \times N}{M} \tag{3}$$

where P is the mass remaining (%) at the above specified mass losses. N is the cycle at which mass loss reaches the above specified values and M is the cycle at which the F-T exposure is to be terminated (56 cycles in this case).

Compressive strength

Compressive strength was measured in accordance with BS EN 12390-3:2009 (British Standards Institution, 2009) on 100 mm cubes at the end of freezing and thawing exposure (56 cycles) at three replicates per mix. An additional three replicates per mix were tested after curing (without exposure to F-T cycles) to act as control references. Samples were placed between two 100 × 100 × 25 mm metal plates and loaded at a rate of 0.3 MPa/s to ultimate failure.

Results and discussion

Mass and area loss

Fig. 3a shows the normalised sample mass (mass in each cycle divided by the initial mass) as a function of F-T cycles for conventional permeable concrete (PC) samples. In the first 10 cycles, only

a slight mass loss occurred. Subsequently, a significant drop in mass occurred as the surface and the edges of the samples deteriorated. Cracking of the cement paste coating lead to debonding of the aggregate particles from the matrix and spalling of the sample (Fig. 4). PC samples with higher porosity showed greater amount of deterioration. The 36% and 37% porosity PC samples deteriorated rapidly until only about 50% of the specimen remained by the end of the F-T exposure (Fig. 3a and 4b). This is due to the pore structure of conventional permeable pavements with higher porosities achieved through a thinner paste layer coating the aggregates, resulting in a lower matrix strength and F-T resistance.

Similarly, a significant loss in surface area was observed beyond the first 10 cycles (Fig. 5a). However, the area loss at each cycle was more significant than the mass loss. Fig. 5b shows the correlation between mass and area remaining at every F-T cycle. The mass and area remaining correlate very well up to cycle 12. However, increasing the number of F-T cycles resulted in more area than mass loss. This is due to PC samples deteriorating from the surface in the form of aggregates loosening and de-bonding from the cement paste before complete spalling.

Fig. 6 presents the durability factor (DF) for a range of mass loss (2%-25%). The DF results clearly showed that at a certain mass loss (e.g. 2%), PC samples of lower porosity provided better F-T durability. This is consistent with the mass loss (Fig. 3a) and area loss (Fig. 5a) data. This is similar to the findings reported by Wu *et al.* (2016), who observed a strong correlation between porosity and durability factor with mixes that have lower porosity showing better F-T durability performance. Liu *et al.* (2018b) have also reported that samples with higher porosity had lower F-T durability.

Unlike PC samples, very little mass loss was observed in CRP samples of different porosity when exposed to F-T cycles (Fig. 3b). Furthermore, the mass loss observed in CRP samples of different porosity (2%-30%) was very similar to the self-compacting mortar samples of 0% porosity. The

durability factor (DF) for all CRP samples were consistently greater than 94%. This is due to the pore structure of CRP that has been engineered to have high permeability, whilst still achieving high strength and F-T durability performance. CRP sample of 30% porosity showed a 6% drop in mass at cycle 56. This was due to spalling of a section of mortar at the boundary between the straight tubes and this was only observed in one of the three replicates. As no deterioration was observed in CRPs of different porosity (Fig. 7), it was decided not to conduct area loss analyses on these samples.

Ultrasonic pulse velocity (UPV)

The freeze-thaw tests were evaluated from the change in mass and area (see 'Mass and area loss' section), and the reduction in ultrasonic pulse velocity (UPV), during F-T exposure. When internal damages start to form within the PC samples, the UPV values decreased (Fig. 8a). This is because the deterioration in PC samples results in an increase in the true path length of the ultrasonic pulse, thus reducing the UPV values with increase in F-T cycles. Samples with higher porosity showed lower UPV values. As no UPV values were detectable from cycle 10 for PC samples of 27%-37% porosity and cycle 17 for PC samples of 16% and 23% porosity, the test was terminated at these cycles.

In contrast, no significant reduction in UPV was observed in the CRP samples of different porosity. As it can be seen in Fig. 8b, the mean UPV value (determined from three replicates; for each replicate UPV is measured at five locations on each side of the cubic sample) of CRP samples of different porosity did not decrease with increase in F-T cycles (on average the % difference in between F-T cycles was less than 1%). The UPV values for CRP samples of 2%-30% porosity were very similar to that in the self-compacting mortar samples of 0% porosity. This highlights the effectiveness of CRP in resisting F-T deterioration, which is attributed to the use of high-strength self-compacting mortar and the engineered vertical pore structure with tortuosity of 1 and no constrictions.

Visual observation of cracking

The PC and CRP samples were scanned after each F-T cycle in order to study the extent of F-T damage. PC samples were found to deteriorate by debonding of aggregate particles due to cracking of the cement paste. The rate of deterioration increased with increase in porosity. In PC samples with porosity greater than 23%, the rate of deterioration at the end of 56 cycles (in the form of loss of aggregate particles and spalling) was so high that it was not possible to carry out further testing (e.g. compressive strength) on the sample (Fig. 4b).

Conversely, the CRP samples of different porosity showed no signs of visible cracking or spalling (Fig. 7). This is attributed to higher cement paste content, the modified pore distribution and the lack of coarse aggregate in CRP. However, there is a possibility that micro cracks are present which are not visible to naked eye. Hence, it would be beneficial to conduct microstructural analysis on future CRP samples. However, as the properties of CRP are unaltered after exposure to 56 F-T cycles, it is believed that these microcracks if exist do not impact the overall durability performance of CRP.

Compressive strength

Porosity and strength are two fundamental properties that closely relate to the durability of permeable concrete pavements. The compressive strength of permeable concrete is influenced by a range of factors including porosity, cement content, w/c ratio, compaction during placement and the characteristics of the aggregate. Fig. 9 presents compressive strength plotted against porosity for all PC and CRP samples. For PC Control samples not exposed to F-T, the compressive strength ranged from 4 MPa to 25 MPa for porosities of 16%-36%. In contrast, the compressive strength of PC samples exposed to F-T cycles (PC F-T) ranged from 0.2 MPa to 7 MPa for porosities of 16%-36%. As expected, strength was inversely proportional to porosity ($R^2 > 0.9$) and on average decreased by about 8% for every 1% increase in porosity. The compressive strength for samples exposed to F-T was 75%-96% lower than the control samples. A strong relationship was observed between

compressive strength and F-T durability. Samples with higher compressive strength (e.g. 16% porosity sample in Fig. 9) exhibited better F-T durability (see Fig. 6), which is consistent with the findings of Wu *et al.* (2016).

The compressive strength for CRP ranged from 12 MPa to 60 MPa for porosities of 2%-30% for both CRP Control and CRP F-T. As expected, compressive strength reduced with increase in porosity for both control and F-T exposed CRP samples. However, it is worth noting that the compressive strength of the control samples was comparable to those samples exposed to 56 F-T cycles. In some cases, the compressive strength of F-T exposed CRP (e.g. 16%, 25%) samples was higher than the CRP Control samples, which indicates that the F-T cycles had no impact on the mechanical properties of CRP. Furthermore, the compressive strength of CRP was substantially higher than the conventional permeable concretes. In fact, at similar porosity, the compressive strength of CRP is about twice that of PC. This is attributed to the difference in pore structure with CRP having a modified pore distribution with higher cement paste content.

Conclusions

The freeze-thaw (F-T) durability of conventional permeable concrete (PC) and high-strength clogging resistant permeable concrete pavement replacement (CRP) was tested and compared. Conventional test methods were used on both permeable pavement systems to compare and determine the F-T durability performance. Some of the key test variables were aggregate particle size (1.25 mm to 14 mm), effective porosity (2% to 37%), pore diameter (3 mm to 6 mm) and freeze-thaw degradation method used to simulate extreme temperature and moisture gradients experienced in the field. The main findings are:

- PC samples of different porosity experienced a significant mass and area loss when exposed to F-T cycles. A significant deterioration of PC samples was observed after 10 cycles in the

form of aggregate loosening due to de-bonding from the cement paste followed by major spalling. This is due to the pore structure of PC consisting of a thin cement paste layer coating the aggregates in order to achieve the required porosity and permeability.

- CRP samples of 2%-30% porosity were more durable to F-T cycles such that no mass loss was observed over the 56 F-T cycles. CRP samples (<30% porosity) showed no signs of cracking or spalling due to their engineered uniform pore structure of low tortuosity.
- The ultrasonic pulse velocity (UPV) values reduced with increase in F-T cycles for PC samples. This was due to deterioration in PC samples resulting in an increase in the ultrasonic pulse path length.
- CRP samples showed superior durability performance when exposed to 56 F-T cycles such that no reduction in UPV values were observed for CRP samples of different porosity.
- Compressive strength decreased by 75%-96% when the PC samples were exposed to F-T. In contrast, the CRP samples showed no signs of deterioration or strength loss when exposed to F-T cycles.

CRP is the first permeable pavement replacement to have high strength, permeability and clogging resistance, whilst being less susceptible to degradation caused by extreme temperature and moisture gradients during freeze-thaw cycles as compared to conventional alternatives. As such, CRP is well suited to address the problems associated with durability of permeable concrete pavements exposed to extreme weather, reducing maintenance requirements and improving sustainability and service-life. A new interlocking tile delivery method, that addresses the challenges of scaling up, has already been developed for CRP and deployed at the new White City Campus of Imperial College London in United Kingdom. Long-term performance monitoring is currently underway and will be reported in due course.

Data availability statement

All experimental and analytical test data used in this study appear in the submitted article.

Acknowledgements

We acknowledge the UK Engineering and Physical Sciences Research Council (EPSRC) for funding this work through the Imperial College London EPSRC Impact Acceleration Account, grant reference number EP/R511547/1. We also thank Mr. Andrew Morris and Dr Marcus Yio for their assistance with the laboratory work.

References

ACI (American Concrete Institute). 2010. *Report on Pervious Concrete*. ACI 522R-10. ACI Committee 522: 1-38.

Amde, A. M. and Rogge, S. 2013. *Development of high quality pervious concrete specifications for Maryland conditions*. MD-13-SP009B4F. Baltimore, MD, USA, State Highway Administration Maryland Department of Transportation.

ASTM International. 2016. ASTM C597-16 Standard Test Method for Pulse Velocity Through Concrete. West Conshohocken, PA, ASTM International.

Attiogbe, E. 1996. "Predicting Freeze-Thaw Durability of Concrete: A New Approach." *ACI Mater. J*. 93 (5), 457–464.

Bilal, H., Chen, T., Ren, M., Gao, X. and Su, A. 2021. "Influence of silica fume, metakaolin & SBR latex on strength and durability performance of pervious concrete." *Constr. Build. Mater*. 275, 122124.

Bonicelli, A., Giustozzi, F. and Crispino, M. 2015. "Experimental study on the effects of fine sand addition on differentially compacted pervious concrete." *Constr. Build. Mater*. 91, 102-110.

British Standards Institution (BSI). 2006. CEN/TR 15177:2006 Testing the freeze-thaw resistance of concrete - Internal structural damage. British Standards Institution.

British Standards Institution (BSI) 2009. BS EN 12390-3:2009 Testing hardened concrete, Part 3: Compressive Strength of Test Samples, British Standards Institution.

British Standards Institution (BSI) 2019. BS ISO 1920-3:2019 Testing of concrete - Part 3: Making and curing test specimens, British Standards Institution.

Chopra, M., Wanielista, M., Ballock, C. and Spence, J. 2007. *Construction and Maintenance Assessment of Pervious Concrete Pavements*. Orlando, FL, U. o. C. F. Stormwater Management Academy: 1-164.

Coughlin, J. P., Campbell, C. D. and Mays, D. C. 2012. "Infiltration and clogging by sand and clay in a pervious concrete pavement system." *J. Hydraul. Eng.* 17 (1), 68-73.

Debnath, B. and Sarkar, P. P. 2020. "Pervious concrete as an alternative pavement strategy: a state-of-the-art review." *Int. J. Pavement Eng.* 21 (12), 1516-1531.

Deo, O., Sumanasooriya, M. and Neithalath, N. 2010. "Permeability reduction in pervious concretes due to clogging: experiments and modeling." *J. Mater. Civ. Eng.* 22 (7), 741-751.

Gesoğlu, M., Güneyisi, E., Khoshnaw, G. and İpek, S. 2014. "Abrasion and freezing–thawing resistance of pervious concretes containing waste rubbers." *Constr. Build. Mater.* 73, 19-24.

Guthrie, W. S., DeMille, C. B. and Eggett, D. L. 2010. "Effects of Soil Clogging and Water Saturation on Freeze–Thaw Durability of Pervious Concrete." *Transp. Res. Rec.* 2164 (1), 89-97.

Henderson, V. and Tighe, S. 2012. "Evaluation of pervious concrete pavement performance in cold weather climates." *Int. J. Pavement Eng.* 13 (3), 197-208.

Huang, J., Valeo, C., He, J. and Chu, A. 2012. "Winter performance of inter-locking pavers - stormwater quantity and quality." *Water.* 4 (4), 995-1008.

Izevbekhai, B. I. and Akkari, A. 2011. *Pervious Concrete Cells on MnROAD Low-Volume Road*. MN/RC 2011-23. St. Paul, MN, USA, Minnesota Department of Transportation.

Jones, D., Harvey, J., Li., H., Wang, R. and Campbell, B. 2010. *Laboratory Testing and Modeling for Structural Performance of Fully Permeable Pavements: Final Report*. 1-214.

411 Kayhanian, M., Anderson, D., Harvey, J. T., Jones, D. and Muhunthan, B. 2012. "Permeability
412 measurement and scan imaging to assess clogging of pervious concrete pavements in parking lots."
413 *J. Environ. Manage.t* 95 (1), 114-123.
414 Kevern, J. T. 2008. *Advancement of pervious concrete durability*, Iowa State University.
415 Kevern, J. T., Schaefer, V. R. and Wang, K. 2009. "Evaluation of pervious concrete workability using
416 gyratory compaction." *J. of Mater. Civ. Eng.* 21, 764–770.
417 Kevern, J. T., Schaefer, V. R., Wang, K. and Suleiman, M. T. 2008a. "Pervious Concrete Mixture
418 Proportions for Improved Freeze-Thaw Durability." *J. ASTM Int.* 5 (2), 1-12.
419 Kevern, J. T., Wang, K. and Schaefer, V. R. 2008b. Pervious Concrete in Severe Exposures. *Concr.*
420 *Int.*. 30, 43-49.
421 Kevern, J. T., Wang, K. and Schaefer, V. R. 2010. "Effect of coarse aggregate on the freeze-thaw
422 durability of pervious concrete." *J. Mater. Civ. Eng.* 22 (5), 469-475.
423 Kia, A., Delens, J. M., Wong, H. S. and Cheeseman, C. R. 2021. "Structural and hydrological design
424 of permeable concrete pavements." *Case Stud. Constr. Mater.* 15, e00564.
425 Kia, A., Wong, H. S. and Cheeseman, C. R. 2017. "Clogging in permeable concrete: A review." *J.*
426 *Environ. Manage.* 193, 221-233.
427 Kia, A., Wong, H. S. and Cheeseman, C. R. 2018. "Defining Clogging Potential for Permeable
428 Concrete." *J. Environ. Manage.* 220, 44-53.
429 Kia, A., Wong, H. S. and Cheeseman, C. R. 2019. "High-Strength Clogging Resistant Permeable
430 Pavement." *Int. J. Pavement Eng.* 2019, 1-20.
431 Kia, A., Wong, H. S. and Cheeseman, C. R. (2020). High strength porous cement-based materials.
432 Kim, H. and Obla, K. H. 2009. *Pervious Concrete: Experimental Validation of Mixture Proportioning*
433 *Methodology*. Silver Spring, MD, N. R. M. C. A. (NRMCA): 1-15.
434 Lian, C. and Zhuge, Y. 2010. "Optimum mix design of enhanced permeable concrete - an
435 experimental investigation." *Constr. Build. Mater.* 24 (12), 2664-2671.

436 Liu, H., Luo, G., Gong, Y. and Wei, H. 2018a. "Mechanical Properties, Permeability, and Freeze–
437 Thaw Resistance of Pervious Concrete Modified by Waste Crumb Rubbers." *Appl. Sci.* 8 (10), 1843.
438 Liu, H., Luo, G., Wei, H. and Yu, H. 2018b. "Strength, Permeability, and Freeze-Thaw Durability of
439 Pervious Concrete with Different Aggregate Sizes, Porosities, and Water-Binder Ratios." *Appl. Sci.*
440 8 (8), 1217.
441 Mata, L. A. and Leming, M. L. 2012. "Vertical distribution of sediments in pervious concrete
442 pavement systems." *ACI Mater. J.* 109 (2), 149-155.
443 Mondal, S. and Biligiri, K. P. 2018. "Crumb Rubber and Silica Fume Inclusions in Pervious Concrete
444 Pavement Systems: Evaluation of Hydrological, Functional, and Structural Properties." *J. Test. Eval.*
445 46 (3), 892-905.
446 NRMCA 2004. *Freeze Thaw Resistance of Pervious Concrete*. MD20910. National Ready Mixed
447 Concrete Association (NRMCA): 1-16.
448 Schaefer, V. R. and Kevern, J. T. 2011. *An Integrated Study of Pervious Concrete Mixture Design*
449 *for Wearing Course Applications*. DTFH61-06-H-00011. Ames, IA, I. S. U. National Concrete
450 Pavement Technology Centre: 1-156.
451 Schaefer, V. R., Wang, K., Suleiman, M. T. and Kevern, J. T. 2006. *Mix Design Development for*
452 *Pervious Concrete In Cold Weather Climates*. Ames, Iowa, USA, Iowa Department of
453 Transportation: 2006-2001.
454 Sonebi, M. and Bassuoni, M. T. 2013. "Investigating the effect of mixture design parameters on
455 pervious concrete by statistical modelling." *Constr. Build. Mater.* 38, 147-154.
456 Sumanasooriya, M. S., Deo, O. and Neithalath, N. 2012. "Particle packing-based material design
457 methodology for pervious concretes." *ACI Mater. J.* 109 (2), 205-213.
458 Sumanasooriya, M. S. and Neithalath, N. 2011. "Pore structure features of pervious concretes
459 proportioned for desired porosities and their performance prediction." *Cem. Concr. Compos.* 33 (8),
460 778-787.

Tennis, P. D., Leming, M. L. and Akers, D. J. 2004. *Pervious Concrete Pavements*. EB302.02. Stokie, Illinois, Portland Cement Association: 1-28.

Wu, H., Liu, Z., Sun, B. and Yin, J. 2016. "Experimental investigation on freeze–thaw durability of Portland cement pervious concrete (PCPC)." *Constr. Build. Mater.* 117, 63-71.

Yang, J. and Jiang, G. 2003. "Experimental study on properties of pervious concrete pavement materials." *Cem. Concr. Res.* 33 (3), 381-386.

Yang, Z. 2011. "Freezing and thawing durability of pervious concrete under simulated field conditions." *ACI Mater. J.* 108 (2), 187-195.

Yang, Z., Brown, H. and Cheney, A. 2006. “Influence of Moisture Conditions on Freeze and Thaw Durability of Portland Cement Pervious Concrete.” In Proc., Concrete Technology Forum: Focus on Pervious Concrete, Nashville, Tennessee.

Yong, C. F., McCarthy, D. T. and Deletic, A. 2013. "Predicting physical clogging of porous and permeable pavements." *J. Hydrol.* 481, 48-55.

Tables

Table 1. Mix proportions of conventional permeable concrete (PC) prepared in the laboratory.

Mix	Cement (kg/m^3)	Gravel (kg/m^3)	Water (kg/m^3)	VMA** (%, kg/m^3)	w/c	Paste vol. (%)	Actual porosity (%)
PC-16%	315	1481	110	-	0.35	21	16
PC-23%	255	1581	89	-	0.35	17	23
PC-27%	255	1581	89	0.3, 0.8	0.35	17	27
PC-29%	255	1581	89	0.2, 0.5	0.35	17	29
PC-29%*	180	1581	63	-	0.35	12	29
PC-36%	105	1581	37	-	0.35	7	36
PC-37%	180	1581	63	0.2, 0.5	0.35	12	37

*Mixes of similar porosity are differentiated by an asterisk.
**VMA refers to viscosity-modifying admixture.

Table 2. Mix compositions of high strength clogging resistant permeable pavement (CRP).

Mix	No of tubes × diameter of tubes (mm) per 100 mm cube sample	Cement (kg/m^3)	Sand (kg/m^3)	Water (kg/m^3)	SP (%)	w/c	Actual porosity (%)
CRP-2%	28 × 3	697	1297	278	0.25	0.4	2
CRP-2%*	8 × 6	697	1297	278	0.25	0.4	2
CRP-4%	56 × 3	683	1270	273	0.25	0.4	4
CRP-4%*	15 × 6	683	1270	273	0.25	0.4	4
CRP-8%	42 × 5	654	1217	261	0.25	0.4	8
CRP-16%	56 × 6	597	1111	239	0.25	0.4	16
CRP-25%	88 × 6	533	992	213	0.25	0.4	25
CRP-30%	105 × 6	498	926	199	0.25	0.4	30

*Mixes of similar porosity are differentiated by an asterisk.

Figures

Fig. 1. *Large-scale delivery of CRP at Imperial College London's White City Campus.*

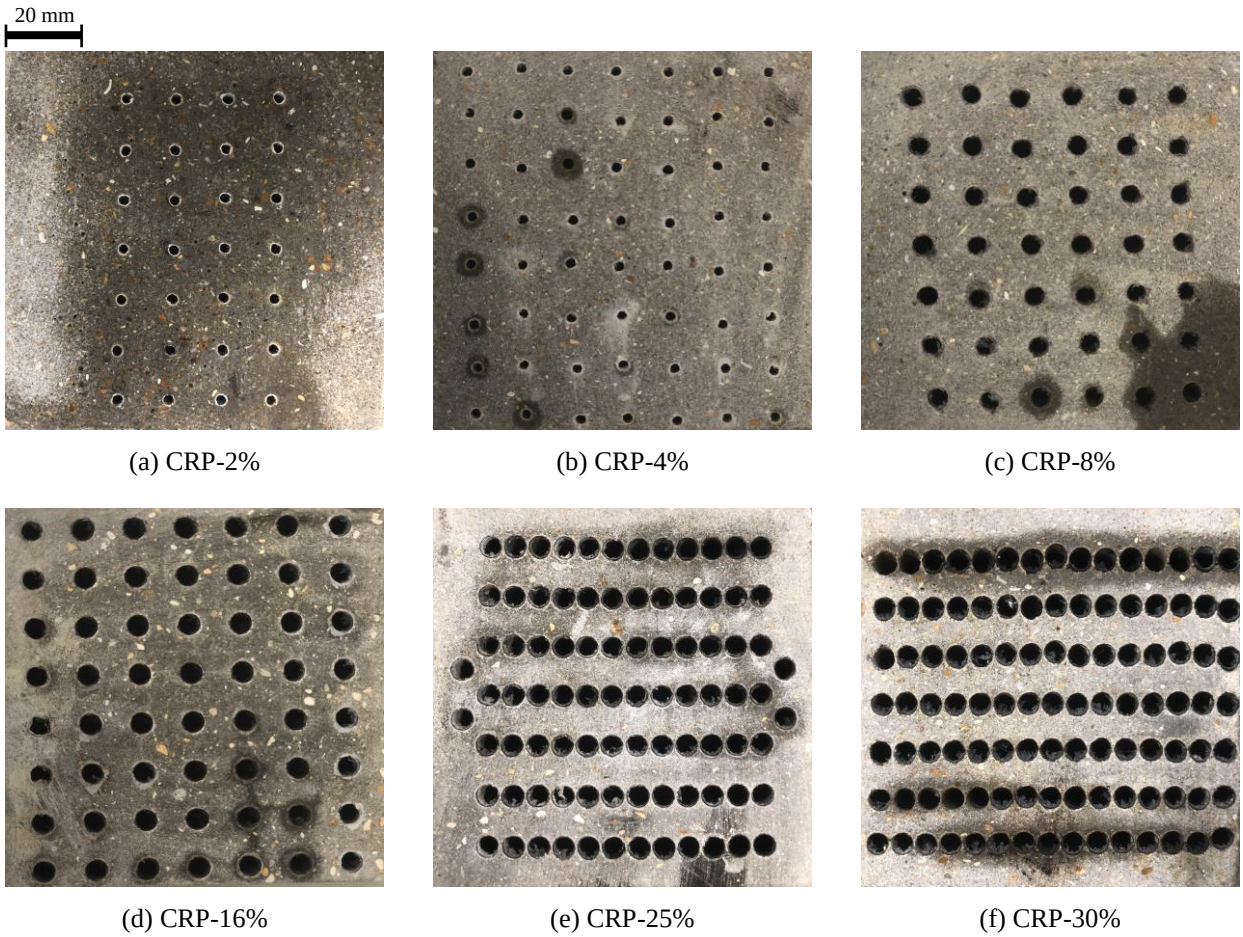

(a) CRP-2% (b) CRP-4% (c) CRP-8%

(d) CRP-16% (e) CRP-25% (f) CRP-30%

Fig. 2. Cross-sections of 100 mm high strength clogging resistant permeable pavement (CRP) containing straight pores of varying size and number in self-compacting mortar to achieve porosity of 2 to 30%.

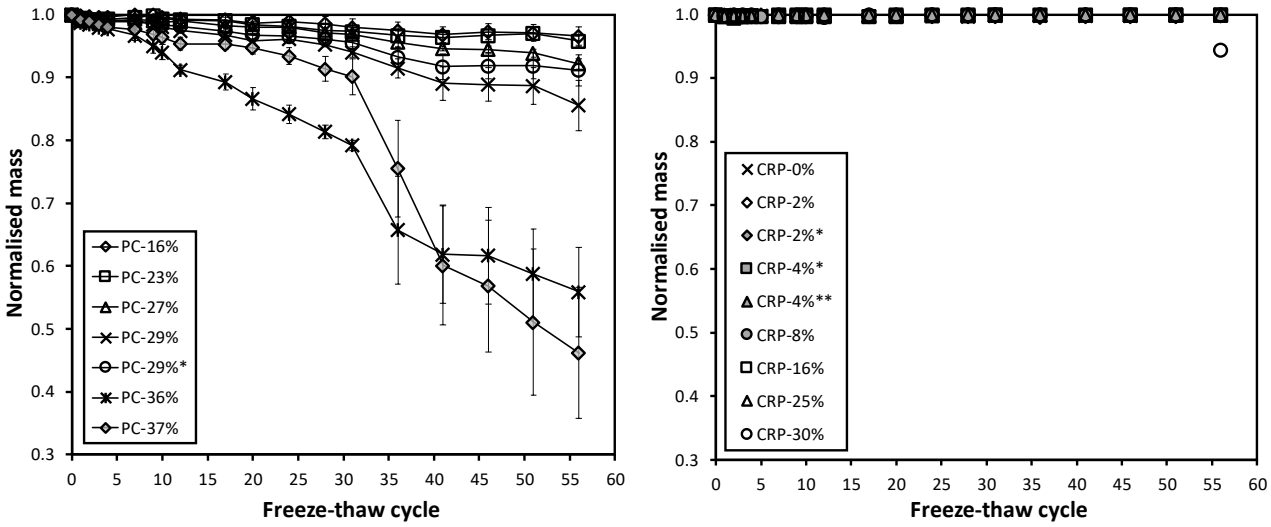

(a) (b)

516 **Fig. 3.** Normalised mass (mass in each cycle divided by the initial mass) against freeze-thaw cycles for a)
517 conventional permeable concrete (PC) and (b) high-strength clogging resistant permeable pavement (CRP).

518
519

(a) PC-16% (b) PC-37%

520 **Fig. 4.** Conventional permeable concrete (PC) at (a) 16% porosity and (b) 37% porosity, shown before and
521 after exposure to 56 F-T cycles, indicating the extent of deterioration.

522
523
524
525
526
527

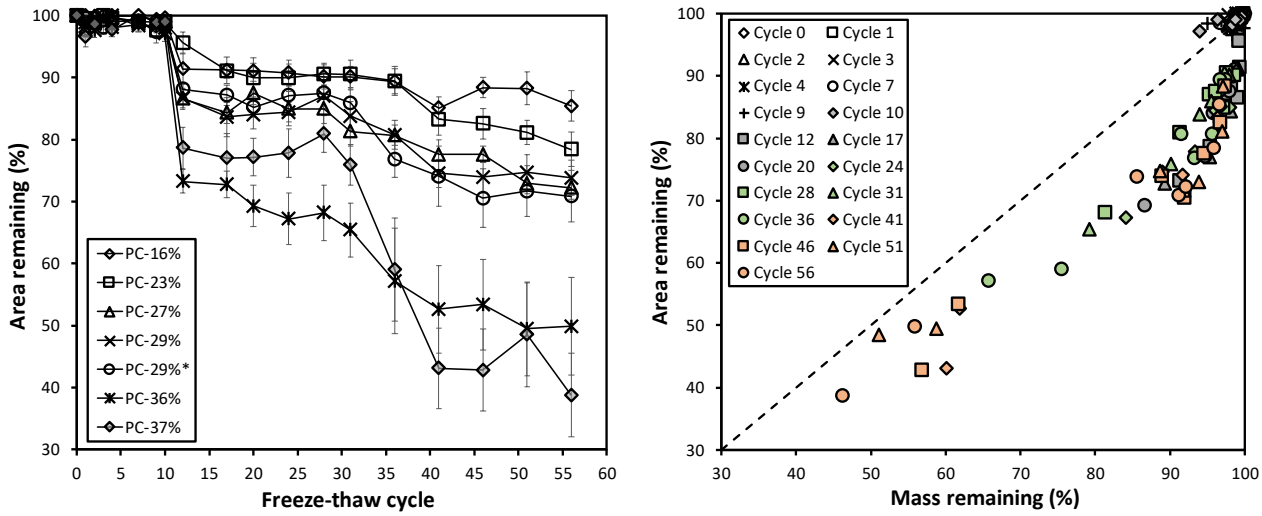

(a) (b)

528 **Fig. 5.** Area remaining against (a) freeze-thaw cycles and (b) mass remaining for conventional permeable
529 concrete (PC) pavement from cycle 0 to 56. A significant drop in area is observed at cycles 12, 36 and 56.

530
531

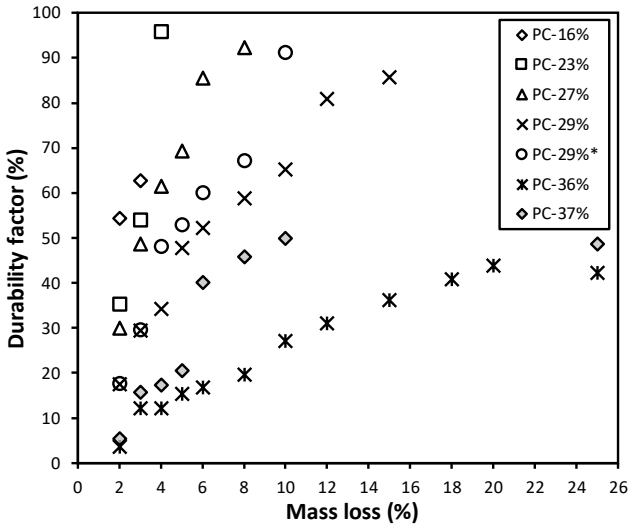

532

533 **Fig. 6.** Durability factor (DF) against varying mass loss for conventional permeable concrete (PC) showing
534 that at a certain mass loss (e.g. 2%), samples with lower porosity have better durability performance.

535
536
537
538
539

(a) CRP-2% (b) CRP-16% (c) CRP-30%

Fig. 7. Clogging resistant permeable pavements (CRP) after exposure to 56 F-T cycles, showing no sign of extensive deterioration.

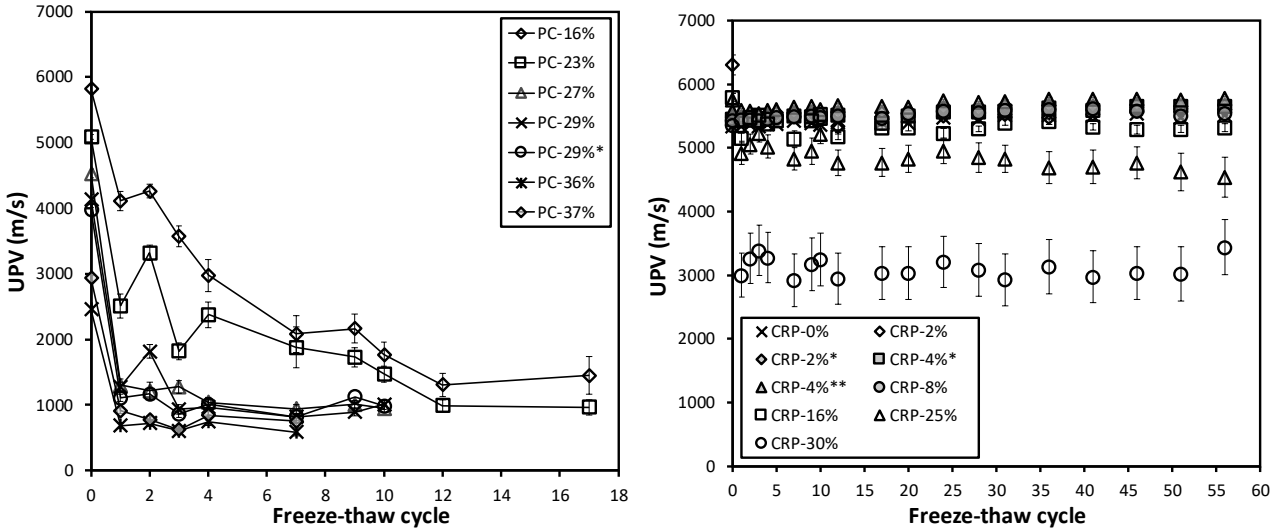

(a) (b)

Fig. 8. Ultrasonic pulse velocity (UPV) against freeze-thaw cycles for (a) conventional permeable concrete (PC) and (b) high-strength clogging resistant permeable pavement (CRP).

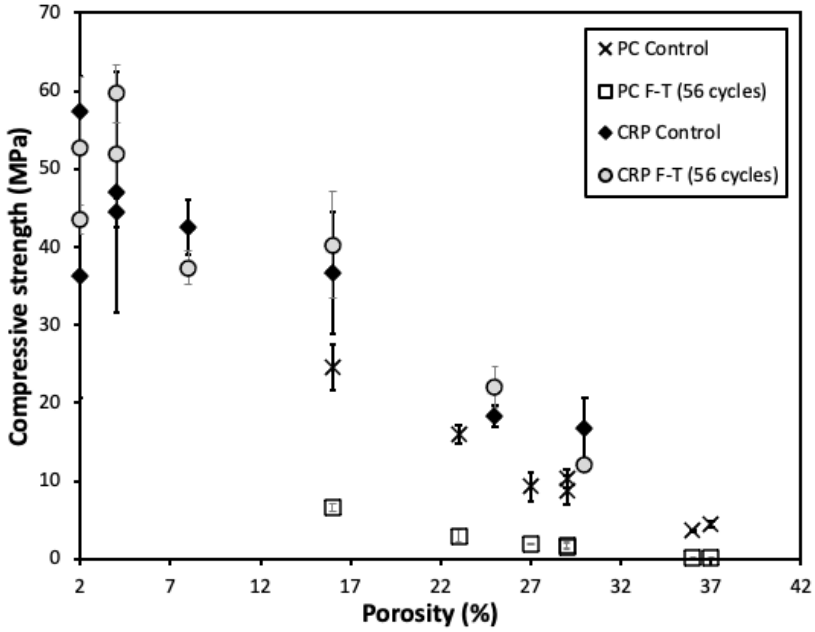

Fig. 9. Correlation between compressive strength and porosity for control samples (PC and CRP) and samples exposed to 56 freeze-thaw cycles (PC F-T and CRP F-T). Conventional permeable concrete (PC) samples show a large drop in compressive strength when exposed to freeze-thaw cycles compared to the CRP samples.